

Using a *quantum work meter* to test non-equilibrium fluctuation theorems

Federico Cerisola,^{1,2} Yair Margalit,³ Shimon Machluf,⁴ Augusto J. Roncaglia,^{1,2} Juan Pablo Paz,^{1,2} and Ron Folman³

¹*Departamento de Física, FCEyN, UBA, Pabellón 1, Ciudad Universitaria, 1428 Buenos Aires, Argentina*

²*Instituto de Física de Buenos Aires, UBA CONICET, Pabellón 1, Ciudad Universitaria, 1428 Buenos Aires, Argentina*

³*Department of Physics, Ben-Gurion University of the Negev, Be'er Sheva 84105, Israel.*

⁴*Van der Waals-Zeeman Institute, University of Amsterdam, Science Park 904, PO Box 94485, 1090 GL Amsterdam, The Netherlands*

(Dated: June 27, 2017)

Non-equilibrium quantum thermodynamics is essential to describe new devices that operate far from the regime where the usual thermodynamical laws are obeyed. When quantum fluctuations dominate, defining and measuring *work* and *heat*, two central concepts in classical thermodynamics, is non-trivial. For driven, but otherwise isolated, quantum systems, work w is a random variable associated with the change in the internal energy, as the first law of thermodynamics indicates. In this paper we present the design and the experimental implementation of a “quantum work meter” (QWM) operating on an ensemble of cold atoms, combining the idea presented in Ref. [1] and the experimental setup used in Ref. [2]. Our QWM not only directly measures work but also directly samples its probability distribution $P(w)$ [i.e. the outcome w is obtained with probability $P(w)$]. As the work probability distribution plays a central role in the fluctuation theorems of non-equilibrium quantum thermodynamics [3–5], the QWM is an ideal tool to test their validity. In particular, we use it to verify the Jarzynski identity [6–10].

Work measurement and the QWM.— A QWM is an apparatus that measures the work performed on a driven quantum system whose Hamiltonian varies from an initial H to a final \tilde{H} with eigenvalues E_n and \tilde{E}_m , respectively. For an isolated system \mathcal{S} , with a D -dimensional space of states, the number of different values of work is bounded by D^2 . Therefore, the pointer of the QWM has D^2 distinct positions (one for each value of $w = w_{nm} = \tilde{E}_m - E_n$). The QWM presented here enables us to choose H and \tilde{H} (fixing the possible values of w) and to vary the intermediate driving (inducing different evolution operators denoted as \mathcal{U}_S). In this way, we vary the probability $P(w)$, which depends on the intermediate driving \mathcal{U}_S .

By sampling $P(w)$, we use the QWM to verify a fundamental result in non-equilibrium quantum thermodynamics: the Jarzynski identity. This establishes a surprising relation between non-equilibrium and equilibrium concepts. The identity states that for any initial thermal state and for any distribution $P(w)$, the linear combination $\langle e^{-\beta w} \rangle = \sum_w e^{-\beta w} P(w)$ is not a non-equilibrium but an equilibrium property, where $\beta = 1/k_B T$ is the in-

verse temperature of the system. The Jarzynski identity (see the Supplementary Material, SM) reads

$$\langle e^{-\beta w} \rangle = e^{-\beta \Delta F}, \quad (1)$$

where ΔF is the free energy difference between the thermal states associated with the Hamiltonians H and \tilde{H} . In the absence of degeneracies, this implies that the vector formed by the $D^2 - 1$ measured probabilities belongs to a $D^2 - 2$ dimensional hyperplane: the “Jarzynski manifold” [as shown in the SM, further constraints restrict this dimensionality to $(D - 1)^2$]. With the QWM we measure $P(w)$ for different driving fields showing that all probability vectors belong to the same manifold. By characterizing this manifold, we not only verify the identity but also independently estimate the free energy difference ΔF [6, 11, 12].

The work distribution sampled by the QWM, introduced in [7–10], is:

$$P(w) = \sum_{n,m} p_n p_{m|n} \delta[w - (\tilde{E}_m - E_n)]. \quad (2)$$

Thus, $P(w)$ is the probability density of finding the energy difference w after a measurement of H followed by an intermediate driving \mathcal{U}_S and a final measurement of \tilde{H} . This is indeed the case if p_n is the probability of obtaining E_n when measuring H and $p_{m|n}$ is the probability of obtaining \tilde{E}_m when measuring \tilde{H} given that E_n was detected at the beginning. Equation (3) defines a probability density that is independent of the initial coherences in the energy basis. For the discrete D^2 values of w we will use $P(w)$ to denote the probability (not the density) of each w . Implementing the two-time-measurement strategy is difficult [13] because the two projective measurements are unavoidably disruptive (see Ref. [14] for an ion trap implementation). Alternative methods to evaluate $P(w)$ relying on the direct estimation of its Fourier transform were proposed in Refs. [15, 16] (and implemented in NMR experiments [17]). Our QWM is conceptually different from previous work-measurement devices. Its main advantage is that the QWM efficiently samples $P(w)$, which is a direct observable in the experiment. The concept on which it is based was discussed in Refs. [1, 18] where it was noticed that the work done on \mathcal{S} , can be detected by performing a generalized quantum

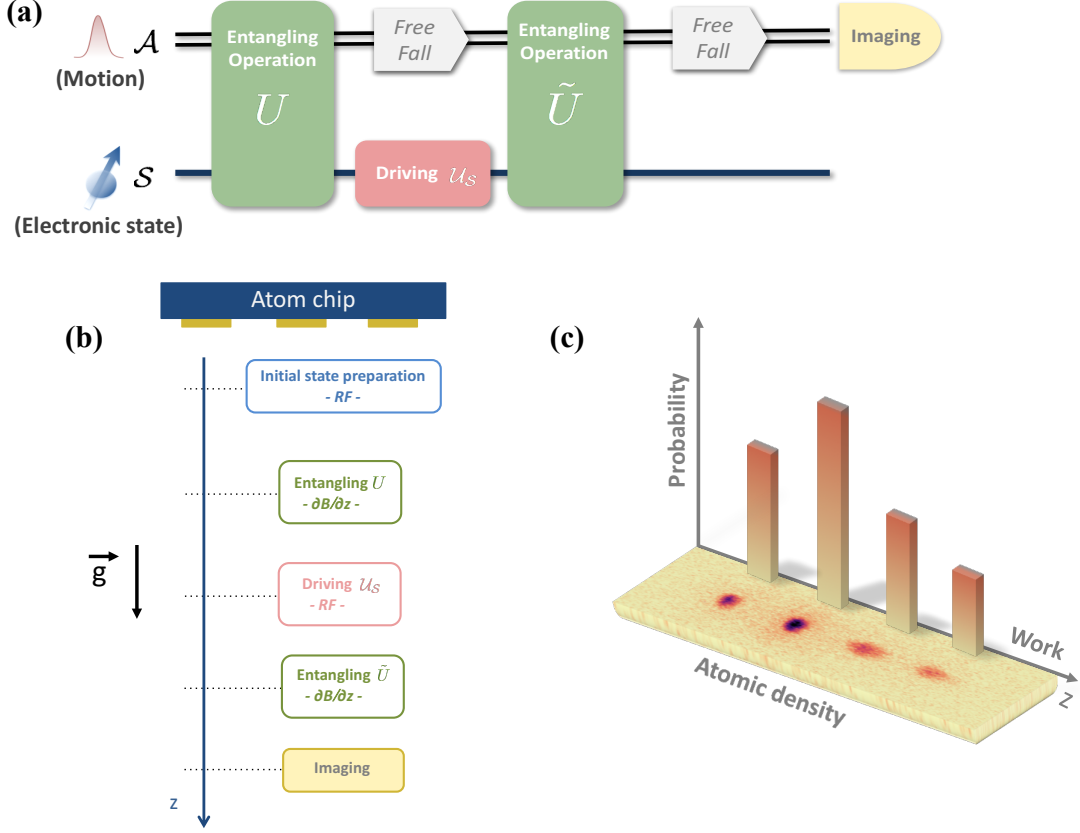


FIG. 1: The QWM. (a) A quantum circuit for the QWM. \mathcal{S} and \mathcal{A} are entangled so that the eigenvalue of the observable H of the system \mathcal{S} is coherently recorded by \mathcal{A} . Then \mathcal{S} is driven by U_S . Finally, another entangling operation between \mathcal{S} and \mathcal{A} creates a record of w on \mathcal{A} . In the experiment, \mathcal{A} is encoded in the motional degree of freedom of the atoms along the vertical direction z , which also evolves while freely falling. \mathcal{S} is the pseudospin associated with two Zeeman sub-levels of a ^{87}Rb atom. (b) Physical operations for the QWM on an atom chip: i) The atoms, prepared in state $|2\rangle$, are released from the trap, and a RF field generates an initial pseudo-thermal state. ii) Internal and motional degrees of freedom are entangled with a magnetic gradient pulse. iii) Another RF field drives \mathcal{S} . iv) A second magnetic gradient pulse is applied. At this stage, \mathcal{A} keeps a record of the different work values. v) The positions and optical densities of the atomic clouds are measured. The number of atoms in each cloud reveals the work probability in a single experimental realisation. (c) Image of the four clouds obtained at the end of a single run of the QWM. The four possible values of w fix the position of each cloud.

measurement, which enables the number of outcomes to be larger than D . This can be done by entangling \mathcal{S} with an ancilla \mathcal{A} that stores a coherent record of w . Then a standard measurement on \mathcal{A} can reveal w .

Design and operation of the QWM—A pictorial representation of the protocol we follow to operate the QWM is shown in Fig. 1a. The QWM is designed to measure the work done on a system \mathcal{S} whose Hamiltonian changes from H to \tilde{H} and which is subjected to a driving U_S in between. We couple \mathcal{S} to a continuous variable system \mathcal{A} and use $\hat{z}_{\mathcal{A}}$ to denote its position (the generator of translations along the momentum p). A coherent record of w is created by an “entangling interaction” between \mathcal{A} and \mathcal{S} that must take place before and after the driving U_S . The unitary operators representing these interactions are: $U = e^{-i\lambda \hat{z}_{\mathcal{A}} \otimes H/\hbar}$ and $\tilde{U} = e^{i\lambda \hat{z}_{\mathcal{A}} \otimes \tilde{H}/\hbar}$, where λ is a coupling parameter. Thus, U and \tilde{U} respectively translate

\mathcal{A} along p by a displacement proportional to $(-\lambda H)$ and $\lambda \tilde{H}$. Then, as shown in the SM, the final measurement of p on \mathcal{A} yields a random result whose distribution $P_{\mathcal{A}}(p)$ is a smeared version of the true work distribution $P(w)$ defined in Eq. (3). In fact, outcome p is obtained with a probability density $P_{\mathcal{A}}(p) = \int dw P(w) f(p - \lambda w)$, where the window function $f(p) = |\langle p|\phi\rangle|^2$ is fixed by $|\phi\rangle$, the initial state of \mathcal{A} [thus, by localizing $|\phi\rangle$ we improve the accuracy in the estimation of $P(w)$].

A “universal” QWM is an apparatus which can measure w and sample $P(w)$ for any possible choice of H and \tilde{H} . To build it, we need enough control to enforce the entangling operators U and \tilde{U} for any choice of H and \tilde{H} . Remarkably, this is achieved for a 2-level system by the atom chip implementation we describe below.

Experimental implementation of the QWM. - To describe our QWM we should identify the physical sys-

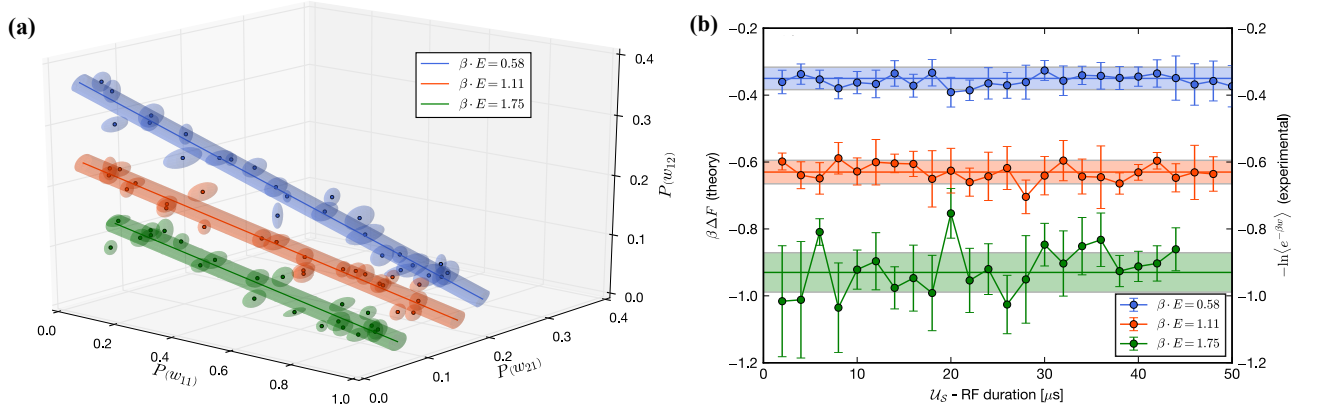


FIG. 2: The Jarzynski identity. **(a)** Each point defines a probability vector (with its experimental error) measured for a certain driving. The three lines correspond to three temperatures: $\beta E = 0.58 \pm 0.02, 1.11 \pm 0.02, 1.75 \pm 0.04$. For each temperature all points lie in the same Jarzynski manifold (which in this case is a line). **(b)** $-\ln\langle e^{-\beta w} \rangle = -\ln[\sum_w e^{-\beta w} P(w)]$ becomes independent of the duration of the intermediate driving (for three temperatures). The dots are the calculated values using the measured work distribution in the Jarzynski identity, and the solid line is the theoretical estimate of $\beta \Delta F$ (with an uncertainty due to the uncertainties in the temperature and energy splitting).

βE	$\beta \Delta F$ (JI)	$\beta \Delta F$ (PF)	$\Delta F/E$ (JI)	$\Delta F/E$ (PF)
0.58 ± 0.02	-0.36 ± 0.04	-0.35 ± 0.03	-0.62 ± 0.07	-0.60 ± 0.06
1.11 ± 0.02	-0.63 ± 0.05	-0.63 ± 0.04	-0.57 ± 0.05	-0.57 ± 0.04
1.75 ± 0.04	-0.92 ± 0.09	-0.93 ± 0.06	-0.53 ± 0.05	-0.53 ± 0.04

TABLE I: Estimates of $\beta \Delta F$ and ΔF for three different temperatures. We show the estimation obtained using the Jarzynski identity (JI) and from a direct calculation of the partition function (PF).

tems representing \mathcal{S} and \mathcal{A} , the way in which H and \tilde{H} can be chosen, and how the associated U and \tilde{U} are implemented. In our experiment we represent \mathcal{S} by the subspace associated with the Zeeman sublevels $|1\rangle \equiv |F=2, m_F=1\rangle$ and $|2\rangle \equiv |F=2, m_F=2\rangle$ of a ^{87}Rb atom that, as in Ref. [2], behaves as a two-level system (see below). The motional degree of freedom of the atom plays the role of \mathcal{A} .

A key element of the QWM presented here is the atom chip [19], which efficiently entangles the internal and motional degrees of freedom of an atom just $\sim 100 \mu\text{m}$ away from the chip surface, through short and strong Stern-Gerlach type magnetic gradient pulses. These pulses are generated using a 3-current-carrying-wire setup on the chip surface (described in Ref. [20] and Methods). A gradient pulse along the z direction with amplitude B' and duration T , induces a momentum kick $m_F \delta p$ on an atom in the m_F state ($\delta p \sim \mu_B g_F B' T$, where μ_B and g_F are, respectively, the Bohr magneton and the Landé factor [2]). The evolution of the state of the atom induced by such a pulse is described by the unitary operator $U_p = e^{i \delta p \hat{z}_A \otimes \hat{\sigma} / \hbar}$, where $\hat{\sigma} = |1\rangle\langle 1| + 2|2\rangle\langle 2|$. This physical operation translates \mathcal{A} along the momentum p by a displacement $\delta p \hat{\sigma}$. As described below, we apply two gradient pulses with different amplitudes (B' and \tilde{B}') and different durations (T and \tilde{T}). Thus, defining $H = E \hat{\sigma}$ and $\tilde{H} = \tilde{E} \hat{\sigma}$, U_p and \tilde{U}_p implement the required

entangling operation U and \tilde{U} , respectively. In this implementation λ is consequently replaced by $-\delta p/E$ and $\delta \tilde{p}/\tilde{E}$, enforcing $\tilde{E}/E = -\delta \tilde{p}/\delta p$. The momentum kicks induced by both pulses are controlled in the experiment, and consequently, by fixing their ratio, we can simulate an arbitrary system with initial and final Hamiltonians H and \tilde{H} which are characterised by \tilde{E}/E having the same ratio. Finally, let us note that the two pulses utilize B' and \tilde{B}' with opposite signs to ensure that the sequence creates a record of work corresponding to $\tilde{E}_m - E_n$.

To achieve universality we only need to be able to fix the energy splitting E and \tilde{E} of H and \tilde{H} , as well as their eigen basis. The traces of H and \tilde{H} (the sum of their eigenvalues) do not affect $P(w)$ but only add a constant to all values of w . As arbitrary E and \tilde{E} can be simulated and any change of basis can be absorbed into U_S , we conclude that our atom chip QWM can sample $P(w)$ for an arbitrary 2-level system and is thus universal.

The ^{87}Rb atoms are magnetically trapped in state $|2\rangle$ and evaporatively cooled to a Bose-Einstein condensation (BEC). The BEC is released from the trap and a radio-frequency (RF) pulse is used to prepare a superposition of $|1\rangle$ and $|2\rangle$. A strong homogeneous magnetic field (created by external coils) suppresses the transitions taking $|1\rangle$ into the $|2, 0\rangle$ state (due to the non-linear Zeeman effect [2]). The initial populations (p_1 and p_2) are chosen so that $\beta E = \ln(p_1/p_2)$ (initial coherences do not

play any role, see SM). The initial motional state is a wave-packet localised in position and momentum.

The experimental sequence, presented in Fig. 1b, is: i) prepare the initial state and release the cloud (which then freely falls along z , the direction of gravity), ii) apply the magnetic gradient U along z , iii) apply the driving \mathcal{U}_S by exposing the atoms to a RF field resonant with the Zeeman splitting induced by the homogeneous bias field, iv) apply the gradient \tilde{U} , v) obtain an image of the four clouds after a time-of-flight and count the number of atoms in each cloud. More details of the experiment can be found in Methods and the SM. For the experimental demonstration presented here we set the ratio between the measured momentum kicks induced by the two pulses to $-\delta\bar{p}/\delta p = 0.56 \pm 0.02$. Hence, our realisation of the QWM samples the work distribution of a simulated system in which the energy splitting is reduced to 56% of its original value, from E to \tilde{E} , while driven by \mathcal{U}_S .

Fig. 1c shows a typical image obtained by the QWM. Four clouds are visible. From the positions of the center of each cloud, \bar{z} , we infer the total momentum shift, \bar{p} , induced by the pulses on that cloud (we take into account both the free fall and the kicks induced by the pulses, see SM). Then, we obtain the corresponding value of work as $w = E \bar{p}/\delta p$ (w is proportional to E , whose value, together with the experimental results, determine the work w). Furthermore, the probability $P(w)$ for each w is directly measured by the number of atoms in each cloud. Notably, this experiment determines the entire $P(w)$ distribution in a single shot.

Testing the Jarzynski identity.— We repeat the experiment fixing the timing, duration and pulse strength. We consider three initial β 's and vary the intermediate driving \mathcal{U}_S by changing the duration of the RF field. In this way, we obtain many sets of probability distributions, each of which defines a $3d$ -vector (as there are three independent probabilities). When we represent all these vectors in the same $3d$ -plot, we see that they all belong to the same β -dependent manifold. Fig. 2a shows that this manifold is a β -dependent line (the dimensionality of this “Jarzynski manifold” is $(D - 1)^2$, which in this case equals 1).

Using the measured work probabilities we calculate the exponential average of the work $\langle e^{-\beta w} \rangle$ for each driving field. Fig. 2b displays the value of $G = -\ln[\langle e^{-\beta w} \rangle] = -\ln[\sum_w e^{-\beta w} P(w)]$ as a function of the duration of the intermediate RF field, that parametrizes \mathcal{U}_S . As established by the Jarzynski identity, G is independent of the driving field and only depends on β . The horizontal lines in Fig. 2b are the theoretically predicted values of $\beta \Delta F$, obtained from a simple calculation (with its own theoretical uncertainty, due to the error in the estimation of βE). We find that, as the Jarzynski identity establishes, $G = \beta \Delta F$.

For $\beta E = 1.75$, we have $P(w) \lesssim 0.1$ for two values of

w and, therefore, the relative error in the atom number estimation is large, inducing a larger error in the estimation of $\beta \Delta F$.

In Table I we compare measured and estimated values of $\beta \Delta F$. The uncertainty in the estimation of $\beta \Delta F$ and ΔF is close to 10%, which is enough to distinguish the three values of $\beta \Delta F$, but leaves a significant overlap for ΔF .

Conclusions.— We presented and implemented a QWM, a new device directly sampling the work distribution on an ensemble of cold atoms. Our QWM can be used to simulate the behavior of an arbitrary 2-level system. We implemented it with an atom chip and verified the Jarzynski identity over a wide range of non-equilibrium processes. This is the first experiment, and so far the only one, directly sampling $P(w)$ offering advantages and different perspectives over previous work measurement schemes. Remarkably, in this cold atom experiment, the QWM extracts full statistical information about the work distribution in a single shot.

Acknowledgments. FC, AJR and JPP acknowledge financial support from ANPCyT (PICT 2013-0621 and PICT 2014-3711), CONICET and UBACyT. YM and RF gratefully acknowledge funding by the Israel Science Foundation, the EC Matter-Wave consortium [FP7-ICT-601180], and the German DFG through the DIP program [FO703/2-1]. SM acknowledges financial support by the Foundation for Fundamental Research on Matter (FOM), which is part of the Netherlands Organisation for Scientific Research (NWO). We also thank the BGU nano-fabrication team for making available the high quality chip, and Zina Binstock for helping with the electronics.

-
- [1] A. J. Roncaglia, F. Cerisola, and J. P. Paz, “Work measurement as a generalized quantum measurement,” *Physical Review Letters*, vol. 113, no. 25, p. 250601, 2014.
 - [2] S. Machluf, Y. Japha, and R. Folman, “Coherent stern-gerlach momentum splitting on an atom chip,” *Nature Communications*, vol. 4, p. 2424, 2013.
 - [3] M. Esposito, U. Harbola, and S. Mukamel, “Nonequilibrium fluctuations, fluctuation theorems, and counting statistics in quantum systems,” *Reviews of Modern Physics*, vol. 81, no. 4, p. 1665, 2009.
 - [4] M. Campisi, P. Hänggi, and P. Talkner, “Colloquium: Quantum fluctuation relations: Foundations and applications,” *Reviews of Modern Physics*, vol. 83, no. 3, p. 771, 2011.
 - [5] U. Seifert, “Stochastic thermodynamics, fluctuation theorems and molecular machines,” *Reports on Progress in Physics*, vol. 75, no. 12, p. 126001, 2012.
 - [6] C. Jarzynski, “Nonequilibrium equality for free energy differences,” *Physical Review Letters*, vol. 78, no. 14, p. 2690, 1997.
 - [7] H. Tasaki, “Jarzynski relations for quantum systems and some applications,” *arXiv preprint cond-mat/0009244*,

- 2000.
- [8] J. Kurchan, “A quantum fluctuation theorem,” *arXiv preprint cond-mat/0007360*, 2000.
 - [9] S. Mukamel, “Quantum extension of the jarzynski relation: analogy with stochastic dephasing,” *Physical Review Letters*, vol. 90, no. 17, p. 170604, 2003.
 - [10] P. Talkner, E. Lutz, and P. Hänggi, “Fluctuation theorems: Work is not an observable,” *Physical Review E*, vol. 75, no. 5, p. 050102, 2007.
 - [11] D. Collin, F. Ritort, C. Jarzynski, S. B. Smith, I. Tinoco, and C. Bustamante, “Verification of the crooks fluctuation theorem and recovery of rna folding free energies,” *Nature*, vol. 437, no. 7056, pp. 231–234, 2005.
 - [12] J. Liphardt, S. Dumont, S. B. Smith, I. Tinoco, and C. Bustamante, “Equilibrium information from nonequilibrium measurements in an experimental test of jarzynski’s equality,” *Science*, vol. 296, no. 5574, pp. 1832–1835, 2002.
 - [13] G. Huber, F. Schmidt-Kaler, S. Deffner, and E. Lutz, “Employing trapped cold ions to verify the quantum jarzynski equality,” *Physical Review Letters*, vol. 101, no. 7, p. 070403, 2008.
 - [14] S. An, J.-N. Zhang, M. Um, D. Lv, Y. Lu, J. Zhang, Z.-Q. Yin, H. Quan, and K. Kim, “Experimental test of the quantum jarzynski equality with a trapped-ion system,” *Nature Physics*, vol. 11, no. 2, pp. 193–199, 2015.
 - [15] L. Mazzola, G. De Chiara, and M. Paternostro, “Measuring the characteristic function of the work distribution,” *Physical Review Letters*, vol. 110, no. 23, p. 230602, 2013.
 - [16] R. Dorner, S. Clark, L. Heaney, R. Fazio, J. Goold, and V. Vedral, “Extracting quantum work statistics and fluctuation theorems by single-qubit interferometry,” *Physical Review Letters*, vol. 110, no. 23, p. 230601, 2013.
 - [17] T. B. Batalhão, A. M. Souza, L. Mazzola, R. Auccaise, R. S. Sarthour, I. S. Oliveira, J. Goold, G. De Chiara, M. Paternostro, and R. M. Serra, “Experimental reconstruction of work distribution and study of fluctuation relations in a closed quantum system,” *Physical Review Letters*, vol. 113, no. 14, p. 140601, 2014.
 - [18] G. De Chiara, A. J. Roncaglia, and J. P. Paz, “Measuring work and heat in ultracold quantum gases,” *New Journal of Physics*, vol. 17, no. 3, p. 035004, 2015.
 - [19] M. Keil, O. Amit, S. Zhou, D. Groswasser, Y. Japha, and R. Folman, “Fifteen years of cold matter on the atom chip: promise, realizations, and prospects,” *Journal of Modern Optics*, vol. 63, no. 18, pp. 1840–1885, 2016.
 - [20] Y. Margalit, Z. Zhou, S. Machluf, D. Rohrlach, Y. Japha, and R. Folman, “A self-interfering clock as a “which path” witness,” *Science*, vol. 349, no. 6253, pp. 1205–1208, 2015.

Methods

Initial state preparation. After preparing the BEC, a homogeneous magnetic field of 36.7 G ($25h\text{ MHz}/\mu_B$) is used to push the transition to $|2, 0\rangle$ out of resonance by $\sim 180\text{ kHz}$ due to the non-linear Zeeman effect, which is larger than the power broadened driving RF field of \mathcal{U}_S . This ensures that the atoms behave as 2-level systems. The BEC is released from the trap and a RF pulse is used to prepare a superposition of $|1\rangle$ and $|2\rangle$. By varying the relative populations we

consider three different pseudo-thermal states. The initial motional state is a wave packet $|\phi\rangle$, well localized at $z_0 = 91 \pm 1.2\ \mu\text{m}$ from the chip and momentum ~ 0 .

Entangling operations and measurement. An inhomogeneous magnetic field is used to couple spin and motional degrees of freedom. This is generated by a current $I = 0.85\text{ A}$ in the 3-wire setup during a time T . The three parallel gold wires lie on the x direction of the chip surface (Fig. 1.b). They are 10 mm long, $40\ \mu\text{m}$ wide and $2\ \mu\text{m}$ thick. Their centers are at $y = -100, 0, 100\ \mu\text{m}$ and the same current run through them in alternating directions ($-I, I, -I$, respectively), creating a 2D quadrupole field at $z = 100\ \mu\text{m}$ below the chip. After a time of flight of 2.4 ms the atoms are at $z \sim 119\ \mu\text{m}$. At this point the first gradient pulse implements U : $T = 40\ \mu\text{s}$ with an amplitude of $B' \sim 95\text{ G/mm}$, such that the momentum kick is along $+z$. Then, after 3.1 ms the atoms are at $\tilde{z} \sim 0.3\text{ mm}$ and the second gradient pulse implements \tilde{U} : $\tilde{T} = 300\ \mu\text{s}$, $\tilde{B}' \sim -7.5\text{ G/mm}$, such that the momentum kick is along $-z$. The relative strengths of the spin-dependent forces sets the energy splitting of the Hamiltonians which in this case is on average $\tilde{E}/E = -\tilde{\delta}p/\delta p = 0.56 \pm 0.02$ (this is the measured value, that takes into account fluctuations in the initial position of the cloud and in the gradient pulses). In between the entangling operation \mathcal{U}_S is applied with a RF pulse. Finally, an image of the atomic clouds is obtained after a time-of-flight of 18.2 ms after the 2nd gradient (the clouds are centered around $z \sim 3\text{ mm}$). The position and number of atoms of each cloud is determined. The momentum shifts of each cloud (that codifies the value of w) are obtained from the difference in positions between the clouds, that follow approximately classical trajectories (see SM).

Uncertainties. The main sources of errors come from the control in the momentum kicks generated by the field gradients (with a fractional uncertainty of 10^{-3}) and also from the errors in the atom counting and the determination of the position for each cloud. Our optical resolution is $\sim 5\ \mu\text{m}$. The central position of each cloud was estimated by fitting a Gaussian profile. Each probability was estimated as a normalized sum of the measured optical density in a relevant region around the cloud. We perform three different runs for each combination of initial state population ratios and intermediate driving and use the average values of position and probability. This gives us a position uncertainty of $\sim 0.015\text{ mm}$ and a probability uncertainty of ~ 0.015 (standard error).

Supplementary Material.

This document is organised as follows. In Section we demonstrate the validity of Jarzynski identity. In Section we briefly review how to measure work by means of a single generalized measurement. In Section we show what is the probability distribution sampled by the QWM and discuss its relation with the true work probability distribution.

Jarzynski identity and quantum work measurement

Work is the energy variation induced on a system \mathcal{S} by a certain driving (the system is otherwise isolated). Suppose that the Hamiltonian of \mathcal{S} changes from an initially H to a final \tilde{H} and that the system is driven by a certain unitary operator \mathcal{U}_S in between. We denote the eigenvalues and eigenvectors of H as E_n and $|\varphi_{n,\alpha}\rangle$ (where α labels different eigenstates with the same energy). In turn the eigenvalues and eigenvectors of \tilde{H} are denoted as \tilde{E}_m and $|\tilde{\varphi}_{m,\gamma}\rangle$ (again, γ labels states with the same energy \tilde{E}_m). Suppose that we measure the energy at the initial and final times. The work probability distribution $P(w)$ is nothing but the probability density to obtain a value w as the difference between the results of the two energy measurements. This can obviously be computed as

$$P(w) = \sum_{n,m} p_n p_{m|n} \delta \left[w - (\tilde{E}_m - E_n) \right], \quad (3)$$

where p_n is the probability of initially measuring energy E_n and $p_{m|n}$ is the probability of measuring energy \tilde{E}_m at the end of the driving given that E_n was detected at the beginning. If the initial state of \mathcal{S} is ρ , the above probabilities can be simply written in terms of the projectors $\Pi_n = \sum_{\alpha} |\varphi_{n,\alpha}\rangle \langle \varphi_{n,\alpha}|$ and $\tilde{\Pi}_m = \sum_{\gamma} |\tilde{\varphi}_{m,\gamma}\rangle \langle \tilde{\varphi}_{m,\gamma}|$. Thus,

$$p_n = \text{Tr}(\rho \Pi_n), \quad p_{m|n} = \frac{1}{p_n} \text{Tr}(\tilde{\Pi}_m \mathcal{U}_S \Pi_n \rho \Pi_n \mathcal{U}_S^\dagger). \quad (4)$$

Jarzynski identity follows immediately from the above definition of the work probability distribution. In fact, if we compute the exponential average of the work, we get

$$\begin{aligned} \langle e^{-\beta w} \rangle &= \int dw P(w) e^{-\beta w} \\ &= \sum_{n,m} p_n p_{m|n} e^{-\beta(\tilde{E}_m - E_n)}. \end{aligned} \quad (5)$$

If the initial state is thermal, then $\rho = \sum_n \Pi_n e^{-\beta E_n} / Z$ (where Z is the partition function $Z = \sum_n g_n e^{-\beta E_n}$ with $g_n = \text{Tr}(\Pi_n)$ being the degeneracy of level E_n). Then, we can replace $p_n = e^{-\beta E_n} / Z$ and perform the summation over the label n by noticing that $\sum_n p_{m|n} = \text{Tr}(\tilde{\Pi}_m) = \tilde{g}_m$. In this way we obtain

$$\langle e^{-\beta w} \rangle = \frac{1}{Z} \sum_m \text{Tr}(\tilde{\Pi}_m) e^{-\beta \tilde{E}_m} = \frac{\tilde{Z}}{Z},$$

where the partition function of the final Hamiltonian is $\tilde{Z} = \sum_m \tilde{g}_m e^{-\beta \tilde{E}_m}$, with $\tilde{g}_m = \text{Tr}(\tilde{\Pi}_m)$ the degeneracy of level \tilde{E}_m . The final step that leads to the Jarzynski identity is simply to notice that for a Gibbs state we have $e^{-\beta \Delta F} = \tilde{Z} / Z$. Thus, the average exponential work becomes independent of the intermediate driving process \mathcal{U}_S and turns out to be determined by equilibrium properties. Thus, $\langle e^{-\beta w} \rangle = e^{-\beta \Delta F}$.

When \mathcal{S} has a finite dimensional Hilbert space, w can only take discrete values. In this case, instead of using the probability density we use directly the probability for each value of w . Thus, we can arrange $P(w)$ as a vector with D^2 components. Taking into account the normalisation condition, the vector of independent probabilities is $D^2 - 1$ dimensional. In turn, being the Jarzynski identity a linear equation in terms of $P(w)$ it constraints the probability vector to belong to a $D^2 - 2$ dimensional hyperplane. But, of course, there are further constraints reducing the number of independent probabilities. The simplest way to obtain this number is to go back to the definition of $P(w)$ in Eq. (3) and count the number of free parameters we have. In this equation, the probabilities p_n are fixed by the initial state. Then, the number of independent probabilities is determined by the number of independent parameters in $p_{m|n}$. For the non-degenerate case we consider here (where all the values of work are different), the calculation is simple. In fact, the coefficients $p_{m|n}$ form a doubly stochastic matrix (since they are all positive numbers such that $\sum_n p_{m|n} = \sum_m p_{m|n} = 1$). For such square matrix of dimension D , there is always $(D - 1)^2$ free parameters. Indeed, this is the dimensionality of the manifold of where the probability vector lies. Jarzynski identity establishes that this manifold is a β -dependent hyperplane (a line in our case, where $D = 2$).

Work measurement as a POVM

Let us consider a system \mathcal{S} with a D -dimensional space of states and show, in a simple way, that the work measurement can be viewed as a generalised quantum measurement. For this, we start by writing the probability for a given value of work $w_{nm} = \tilde{E}_m - E_n$ as

$$P(w_{nm}) = p_{m|n} p_n. \quad (6)$$

Using the formula for the transition probability, we find that

$$P(w_{nm}) = \text{Tr}(\tilde{\Pi}_m \mathcal{U}_S \Pi_n \rho \Pi_n \mathcal{U}_S^\dagger) = \text{Tr}(\rho A_{nm}), \quad (7)$$

where

$$A_{nm} = \Pi_n \mathcal{U}_S^\dagger \tilde{\Pi}_m \mathcal{U}_S \Pi_n. \quad (8)$$

It is simple to verify that the operators A_{nm} expand the identity as $\mathbb{I} = \sum_{n,m} A_{nm}$ and that they are positive semi-definite (i.e., that for any state $|\chi\rangle$ we have $\langle \chi | A_{nm} | \chi \rangle \geq 0$). Therefore, the operators A_{nm} define a positive operator valued measure (POVM), which is the most general type of measurement one can perform in quantum mechanics. Therefore, work can be measured in the same way as any POVM can: A powerful result (Neumark's theorem) establishes that any POVM can be realised by coupling the system \mathcal{S} with an ancillary system \mathcal{A} and then performing a standard projective measurement on \mathcal{A} . This measurement can be performed at a single time. Thus, surprisingly, the two-time work measurement strategy can be replaced by a single-time strategy (which is the basic idea exploited by our QWM). In the following section we show how one can construct an approximation for that ideal apparatus, that we call Quantum Work Meter (QWM).

Probability distribution for the outcome of a QWM

Here we compute the probability distribution for the result of the measurement of the auxiliary register of a general Quantum Work Meter. The protocol defining the apparatus is shown in Figure 1 of the main text. A system \mathcal{S} is coupled to an ancillary one \mathcal{A} . This ancilla is a continuous variable system (of course this can be relaxed). The system \mathcal{S} and the ancilla \mathcal{A} are subject to the following evolution: *i*) an entangling interaction U is applied (which correlates \mathcal{S} and \mathcal{A}), *ii*) the evolution \mathcal{U}_S is applied on the system \mathcal{S} , *iii*) a second entangling interaction \tilde{U} is applied. Finally, after this sequence \mathcal{A} is measured. The initial state of the system formed by \mathcal{S} will be assumed to be a product state. For simplicity, we first assume that the states are pure and denote them as $|\xi\rangle$ (the state of \mathcal{S}) and $|\phi\rangle$ (the state of \mathcal{A}). We will later generalise the result for an initial state which is a tensor product of arbitrarily mixed states. After the sequence of operations we described above, the total final state is:

$$|\Phi(t_f)\rangle = \tilde{U} (I_{\mathcal{A}} \otimes \mathcal{U}_S) U |\phi\rangle \otimes |\xi\rangle$$

The nature of the two entangling operations, that was discussed in the main text, is such that they both induce translations of \mathcal{A} which depend on the state of \mathcal{S} . More specifically, $U = e^{-\frac{i}{\hbar} \lambda \hat{z}_{\mathcal{A}} \otimes H}$ and $\tilde{U} = e^{\frac{i}{\hbar} \lambda \hat{z}_{\mathcal{A}} \otimes \tilde{H}}$, where we use $\hat{z}_{\mathcal{A}}$ to denote the generator of translations of \mathcal{A} along a certain variable p . Using this, it is simple to rewrite the final state as

$$|\Phi(t_f)\rangle = \sum_{n,m} D_{nm} |\phi\rangle \otimes \tilde{\Pi}_m \mathcal{U}_S \Pi_n |\xi\rangle$$

In this equation the displacement operators D_{nm} act on the states of \mathcal{A} and are defined as $D_{nm} = e^{\frac{i}{\hbar} \lambda w_{nm} \hat{z}_{\mathcal{A}}}$.

The interpretation of the above equation is simple: After the sequence of operations, \mathcal{S} and \mathcal{A} become entangled in such a way that a record of w_{nm} is stored in \mathcal{A} . The states $|F_{nm}\rangle \equiv D_{nm} |\phi\rangle$ are “flag states” associated with the different values of work. When these states are orthogonal, they can be unambiguously distinguished and the value of work can be retrieved. Below, we will consider a more realistic scenario where the initial state of \mathcal{A} is a localised coherent state. In that case, the flag states are displaced coherent states (which are simply translated along the variable p direction by an amount that is proportional to w_{nm}). These states are not strictly orthogonal, but have a finite overlap. This induces an error in the work estimation protocol. However, the error can be exponentially reduced by simply increasing the interaction strength λ (as the overlap exponentially decreases with λ).

From the above expression it is simple to obtain the quantum state of \mathcal{A} by computing its reduced density matrix (which is obtained from the total state by tracing out the system \mathcal{S}). Thus,

$$\rho_{\mathcal{A}}(t_f) = \sum_{n,n',m} \text{Tr} \left(\tilde{\Pi}_m \mathcal{U}_{\mathcal{S}} \Pi_n |\xi\rangle \langle \xi| \Pi_{n'} \mathcal{U}_{\mathcal{S}}^\dagger \right) D_{nm} |\phi\rangle \langle \phi| D_{n'm}^\dagger. \quad (9)$$

This expression can be generalised to the case where the initial states of \mathcal{S} and \mathcal{A} are initially mixed. In fact, if $\rho_{\mathcal{S}}$ and $\rho_{\mathcal{A}}$ respectively denote the initial density matrices of \mathcal{S} and \mathcal{A} , the final state of \mathcal{A} is

$$\rho_{\mathcal{A}}(t_f) = \sum_{n,n',m} \text{Tr} \left(\tilde{\Pi}_m \mathcal{U}_{\mathcal{S}} \Pi_n \rho_{\mathcal{S}} \Pi_{n'} \mathcal{U}_{\mathcal{S}}^\dagger \right) D_{nm} \rho_{\mathcal{A}} D_{n'm}^\dagger. \quad (10)$$

From the above equation we obtain the probability density for detecting the value p in a measurement of \mathcal{A} . Thus,

$$P_{\mathcal{A}}(p) = \sum_{n,n',m} \text{Tr} \left(\tilde{\Pi}_m \mathcal{U}_{\mathcal{S}} \Pi_n \rho_{\mathcal{S}} \Pi_{n'} \mathcal{U}_{\mathcal{S}}^\dagger \right) \langle p - \lambda w_{nm} | \rho_{\mathcal{A}} | p - \lambda w_{n'm} \rangle. \quad (11)$$

The contribution of the diagonal ($n = n'$) and off-diagonal ($n \neq n'$) terms play a different role in the above expression. In fact, it is simple to show that the diagonal contribution is a smeared version of the true work distribution. Thus,

$$\sum_{n,m} \text{Tr} \left(\tilde{\Pi}_m \mathcal{U}_{\mathcal{S}} \Pi_n \rho_{\mathcal{S}} \Pi_n \mathcal{U}_{\mathcal{S}}^\dagger \right) \langle p - \lambda w_{nm} | \rho_{\mathcal{A}} | p - \lambda w_{nm} \rangle = \int dw P(w) f(p - \lambda w), \quad (12)$$

where the window function is

$$f(p) = \langle p | \rho_{\mathcal{A}} | p \rangle. \quad (13)$$

Therefore, the off-diagonal terms of $\rho_{\mathcal{S}}$ are responsible for the error in the work estimation and should be made small for it to be accurate. It is simple to show that if the momentum wave function of the initial state $|\phi\rangle$ is a Gaussian with a momentum dispersion $1/\sigma$ (σ is the position dispersion), then the off-diagonal terms are bounded by:

$$\left| \sum_{n \neq n',m} \text{Tr} \left(\tilde{\Pi}_m \mathcal{U}_{\mathcal{S}} \Pi_n \rho_{\mathcal{S}} \Pi_{n'} \mathcal{U}_{\mathcal{S}}^\dagger \right) \langle p - \lambda w_{nm} | \phi \rangle \langle \phi | p - \lambda w_{n'm} \rangle \right| \leq \sum_{n \neq n',m} \left| \text{Tr} \left(\tilde{\Pi}_m \mathcal{U}_{\mathcal{S}} \Pi_n \rho_{\mathcal{S}} \Pi_{n'} \mathcal{U}_{\mathcal{S}}^\dagger \right) \right| \frac{\sigma}{\hbar \sqrt{\pi}} e^{-\frac{\sigma^2 \lambda^2}{4 \hbar^2} (E_n - E_{n'})^2}$$

Thus, by increasing λ (the interaction strength) or σ (the position dispersion of the initial state) we exponentially reduce the error in the work estimation. It is worth noting that by increasing σ we reduce the momentum uncertainty and localise the initial state in momentum. Naturally, the method becomes precise when the initial localisation in momentum is much smaller than the difference between the first momentum kicks (which is fixed by the product $\lambda(E_n - E_{n'})$). When these conditions are satisfied, the off-diagonal terms can be neglected and the probability density to detect p is

$$P_{\mathcal{A}}(p) = \int dw P(w) f(p - \lambda w),$$

where the window function $f(p)$ is defined as $f(p) = |\langle p | \phi \rangle|^2$ (which, for a coherent state is simply $f(p) = e^{-\frac{\sigma^2}{\hbar^2} p^2} \sigma / \hbar \sqrt{\pi}$).

QWM using an atom chip

Here we consider the implementation of the QWM using a cloud of atoms in a chip. As described in the main text, \mathcal{S} is the pseudo spin $1/2$ associated with the $F = 2$, $m_F = 1, 2$ hyperfine states of a ^{87}Rb atom (which, as discussed in the main text, behaves as a two level atom). \mathcal{A} is encoded in the motional degrees of freedom of each atom. There are two subtle differences between the ideal protocol for a QWM described in the previous section and the implementation in an atom chip. The first different concerns the final measurement. Thus, in the previous section we computed the probability for a final momentum measurement but in the real experiment we are forced to measure the atomic position by taking an image of the atomic clouds. Therefore we will show below that the position

measurement enables us to determine work and sample $P(w)$. The second difference is that in the real experiment we should take into account the fact that the ancilla \mathcal{A} evolves during the whole process because the atoms actually move (they freely fall along the vertical direction). Thus, the real protocol describing the experiment is shown in Fig. 3.

Let us now analyse this process. We can first neglect the free fall taking place between the two entangling operations (we take this into account later) and assume the initial state of \mathcal{A} is a coherent state localised around initial values of position and momentum which we arbitrarily take as $z = 0$ and $p = 0$. We denote this state as $|\phi\rangle = |0, 0\rangle$. The calculation presented in the above section should be slightly modified. In this case the flag states are $|F_{nm}\rangle = u_{fall}^{(1)} D_{nm} |0, 0\rangle$. Taking into account that $u_{fall} = e^{-\frac{i}{\hbar} t (\hat{p}_A^2 / 2m_a - m_a g \hat{z}_A)}$ (where t is the duration of the free-fall, m_a is the mass of the atoms, and g the gravity acceleration) we can easily compute the expectation value of the position for each flag state (as well as the corresponding position dispersion). In fact, we have

$$z_{nm}(t) = -w_{nm} \frac{\lambda t}{m_a} + \frac{g}{2} t^2 \quad \text{and} \quad \Delta z_t = \frac{\sigma}{\sqrt{2}} \sqrt{1 + \left(\frac{\hbar t}{m_a \sigma^2} \right)^2}. \quad (14)$$

Therefore, we can notice that by measuring the final position of the atoms we can infer the value of the momentum before the fall and thus acquire information about work w . In fact, the difference between the positions of the clouds is proportional to the difference in the values of work. The price we have to pay, is that the spread of the wave packets increases during the free-fall.

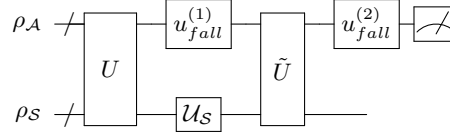


FIG. 3: Set of gates describing the atom chip QWM. $u_{fall}^{(1)}$ and $u_{fall}^{(2)}$ are the free fall evolution that the atoms feel during the experiment. Finally there is a measurement of the position of the atoms.

In a more realistic description of the experiment, we need to include also the free fall between the entangling gates ($u_{fall}^{(1)}$ in Fig. 3). It is easy to verify that since $u_{fall}^{(1)} \hat{z}_A u_{fall}^{(1)\dagger} = \hat{z}_A + \hat{p}_A t / m_a + \mathbb{I}_A g t^2 / 2$ (where t is the duration of the free fall), then $u_{fall}^{(1)} e^{\frac{i}{\hbar} \lambda \hat{z}_A \otimes \tilde{H}} u_{fall}^{(1)\dagger} = e^{\frac{i}{\hbar} \lambda \hat{z}_A \otimes \tilde{H}} e^{\frac{i}{\hbar} \frac{t}{m} \lambda \hat{p}_A \otimes \tilde{H}} e^{\frac{i}{\hbar} \theta \mathbb{I}_A \otimes \tilde{H}}$. Thus, the first term is the usual entangling operation and the last term is just a phase depending on the value of the energy. In turn, the second term is an entangling operation where the atom is displaced along position (instead of momentum) depending on the state of \mathcal{S} . In summary, the free-fall in between the entangling gates simply induces an extra translation of the atoms by an amount that depends on the final value of the energy.